Published OnlineFirst September 16, 2011; DOI: 10.1158/1535-7163.MCT-11-0264

Preclinical Development

Molecular Cancer Therapeutics

Cabozantinib (XL184), a Novel MET and VEGFR2 Inhibitor, Simultaneously Suppresses Metastasis, Angiogenesis, and Tumor Growth

F. Michael Yakes, Jason Chen, Jenny Tan, Kyoko Yamaguchi, Yongchang Shi, Peiwen Yu, Fawn Qian, Felix Chu, Frauke Bentzien, Belinda Cancilla, Jessica Orf, Andrew You, A. Douglas Laird, Stefan Engst, Lillian Lee, Justin Lesch, Yu-Chien Chou, and Alison H. Joly

Abstract

The signaling pathway of the receptor tyrosine kinase MET and its ligand hepatocyte growth factor (HGF) is important for cell growth, survival, and motility and is functionally linked to the signaling pathway of VEGF, which is widely recognized as a key effector in angiogenesis and cancer progression. Dysregulation of the MET/VEGF axis is found in a number of human malignancies and has been associated with tumorigenesis. Cabozantinib (XL184) is a small-molecule kinase inhibitor with potent activity toward MET and VEGF receptor 2 (VEGFR2), as well as a number of other receptor tyrosine kinases that have also been implicated in tumor pathobiology, including RET, KIT, AXL, and FLT3. Treatment with cabozantinib inhibited MET and VEGFR2 phosphorylation *in vitro* and in tumor models *in vivo* and led to significant reductions in cell invasion *in vitro*. In mouse models, cabozantinib dramatically altered tumor pathology, resulting in decreased tumor and endothelial cell proliferation coupled with increased apoptosis and dose-dependent inhibition of tumor growth in breast, lung, and glioma tumor models. Importantly, treatment with cabozantinib did not increase lung tumor burden in an experimental model of metastasis, which has been observed with inhibitors of VEGF signaling that do not target MET. Collectively, these data suggest that cabozantinib is a promising agent for inhibiting tumor angiogenesis and metastasis in cancers with dysregulated MET and VEGFR signaling. *Mol Cancer Ther; 10(12); 2298–308. ©2011 AACR.*

Introduction

The receptor tyrosine kinase MET is the only known receptor for hepatocyte growth factor (HGF), and its signaling activity is required for embryogenesis, cell proliferation, survival, and motility (1). While MET and HGF are found in low levels in normal adult tissues, their expression is frequently dysregulated in a broad spectrum of human tumors. Ectopic activation of MET promotes tumor cell survival, growth, angiogenesis, invasion, and metastasis (2, 3). In preclinical animal models, overexpression of MET and/or HGF has been shown to stimulate tumorigenesis and metastasis (2, 4), whereas downregulation of MET or HGF expression resulted in increased apoptosis and decreased tumor growth and blood vessel density (5, 6). Clinically, dysregulated expression of HGF and/or MET has been observed in many different tumor types, including glioma, melanoma, hepatocellular, renal, gastric, pancreatic, prostate, ovarian, breast, and lung cancers, and is often correlated with poor prognosis (1, 7). Collectively, these observations strongly implicate MET/HGF signaling in the pathogenesis of human cancer.

Induction of angiogenesis has been increasingly recognized as a crucial step in tumor progression and is one of the hallmarks of cancerous growth. Correspondingly, the proangiogenic signaling molecule VEGF and its receptors VEGFR1, VEGFR2, and VEGFR3 play key roles in tumor development. HGF is also a potent angiogenic factor and acts synergistically with VEGF to induce angiogenesis (8, 9). The U.S. Food and Drug Administration-approved VEGF pathway inhibitors bevacizumab, sunitinib, and sorafenib have proven to be clinically important in the treatment of many types of cancer, but their effects are characterized by initial clinical benefit lasting weeks or months before the resumption of tumor growth and progression (10–12). Preclinical studies have found that while continuous VEGF pathway inhibition initially slows tumor growth and trims tumor vasculature, this is quickly followed by rapid revascularization and increased tumor invasiveness (13). These observations show that cancers have the capacity to develop resistance to VEGF pathway–targeted inhibition.

Authors' Affiliation: Exelixis, Inc., South San Francisco, California

Note: Supplementary material for this article is available at Molecular Cancer Therapeutics Online (http://mct.aacrjournals.org/).

Corresponding Author: F. Michael Yakes, Exelixis, Inc., 210 East Grand Ave, South San Francisco, CA 94083. Phone: 650-837-7253; Fax: 650-837-8315; E-mail: myakes@exelixis.com

doi: 10.1158/1535-7163.MCT-11-0264

Published OnlineFirst September 16, 2011; DOI: 10.1158/1535-7163.MCT-11-0264

Tumor cell evasion of VEGF pathway–targeted inhibition may occur as a response to hypoxia. Under hypoxic conditions, hypoxia-inducible factor 1α is upregulated, resulting in increased expression of both VEGF and MET (14, 15). These responses apparently allow the tumor cells to compensate for the hypoxic environment through stimulation of angiogenesis or migration away from the hypoxic zone. Because VEGF pathway inhibition can result in induction of hypoxia, it may also trigger upregulation of MET expression, which may then stimulate tumor invasion. Indeed, Shojaei and colleagues recently determined that the MET pathway plays an important role in the development of resistance to VEGF pathway inhibition by sunitinib treatment (16). Recent studies have also showed that the use of VEGFR inhibitors, such as sunitinib, sorafenib, cediranib, or a VEGFR2-targeting antibody, can result in the development of an aggressive tumor phenotype characterized by increased invasiveness and metastasis and, in patients treated with cediranib, higher MET expression levels (17–19). Therefore, targeting both arms of the MET/VEGF axis simultaneously may critically disrupt angiogenesis, tumorigenesis, and cancer progression.

Cabozantinib (XL184) is a potent inhibitor of MET and VEGFR2 that also inhibits RET, KIT, AXL, and FLT3, all of which have been implicated in tumor pathogenesis (20, 21). In this study, we report on the consequences of cabozantinib treatment on angiogenesis, cellular invasion, tumor growth, and metastasis. Collectively, these data suggest that cabozantinib may provide enhanced efficacy by simultaneously targeting key pathways important to tumor survival, metastasis, and angiogenesis.

Materials and Methods

Compounds

Cabozantinib (Fig. 1A) was synthesized as described in US Patent 7579473 (WO 2005030140 A2; ref. 22). For *in vitro* assays, 10 mmol/L cabozantinib was prepared in dimethyl sulfoxide and serially diluted in the appropriate assay media. For *in vivo* studies, cabozantinib was formulated in sterile saline/10 mmol/L HCl or in water and administered via oral gavage at 10 mL/kg (mice) or 2 mL/kg (rats).

Kinase inhibition assays

The inhibition profile of cabozantinib against a broad panel of 270 human kinases was determined using luciferase-coupled chemiluminescence, ^{33}P-phosphoryl transfer, or AlphaScreen technology (PerkinElmer). Recombinant human full-length, glutathione *S*-transferase tag, or histidine tag fusion proteins were used, and half maximal inhibitory concentration (IC_{50}) values were determined by measuring phosphorylation of peptide substrate poly (Glu, Tyr) at ATP concentrations at or below the K_m for each respective kinase. The mechanism of kinase inhibition was evaluated using the AlphaScreen Assay by determining the IC_{50} values over a range of ATP concentrations.

Cell lines

A431, B16F10, C6, H441, H69, Hs746T, HT1080, MS1, PC3, SNU-1, SNU-5, SNU-16, and U87MG cells were purchased from the American Type Culture Collection, BaF3 cells were purchased from the German Resource Center for Biological Material (DSMZ), and HMVEC-L cells were purchased from BioWhitttaker Technologies. MDA-MB-231 cells were a gift from Georgetown University School of Medicine, Washington, DC. No further authentication was done on these lines. Cell lines were passaged for less than 3 months and maintained in either Dulbecco's Modified Eagle's Media (DMEM) or RPMI-1640 media supplemented with 10% FBS, 1% penicillin-streptomycin, and 1% nonessential amino acids at 37°C in 5% CO_2. Where indicated, assays were conducted using parental cell lines stably transfected with expression vectors encoding kinases of interest.

Inhibition of receptor phosphorylation

Receptor phosphorylation of MET, VEGFR2, AXL, FLT3, and KIT were, respectively, assessed in PC3, HUVEC, MDA-MB-231, FLT3-transfected BaF3, and KIT-transfected MDA-MB-231 cells. Cells were serum starved for 3 to 24 hours, then incubated for 1 to 3 hours in serum-free medium with serially diluted cabozantinib before 10-minute stimulation with ligand: HGF (100 ng/mL), VEGF (20 ng/mL), SCF (100 ng/mL), or ANG1 (300 ng/mL). All ligands were purchased from R&D Systems. Receptor phosphorylation was determined either by ELISA using specific capture antibodies and quantitation of total phosphotyrosine (Zymed, Inc.) or immunoprecipitation and Western blotting with specific antibodies and quantitation of total phosphotyrosine (4G10; UpState Biotechnology). Total protein served as loading controls.

Endothelial cell tubule formation assays

Human microvascular endothelial cells (HMVEC) were mixed with serially diluted cabozantinib, then immediately added to cultures of normal human diploid fibroblasts in the presence or absence of 60 ng/mL VEGF for 7 days. Conditioned media from MDA-MB-231, A431, HT1080, and B16F10 cells were also used as a source of secreted growth factors. Following fixation, tubule formation was detected using the endothelial cell marker CD31 (clone WM59; BD Biosciences) and visualized with an immunoperoxidase detection system (Artisan AEC Detection Kit; Dako). Digital images were captured using an inverted microscope (×20), and total tube length was quantitated with Metamorph (Molecular Devices).

Invasion and migration assays

B16F10 cells (2×10^5) were seeded onto 0.8 μm membranes in the upper chambers of a 96-well Transwell plate in the absence or presence of Matrigel (BD Pharmingen; BD Biosciences). Cells were incubated with serially diluted cabozantinib in DMEM/0.1% FBS. The lower chambers contained HGF (50 ng/mL) and the appropriate concentration of cabozantinib. After 24 hours, cells were

Published OnlineFirst September 16, 2011; DOI: 10.1158/1535-7163.MCT-11-0264

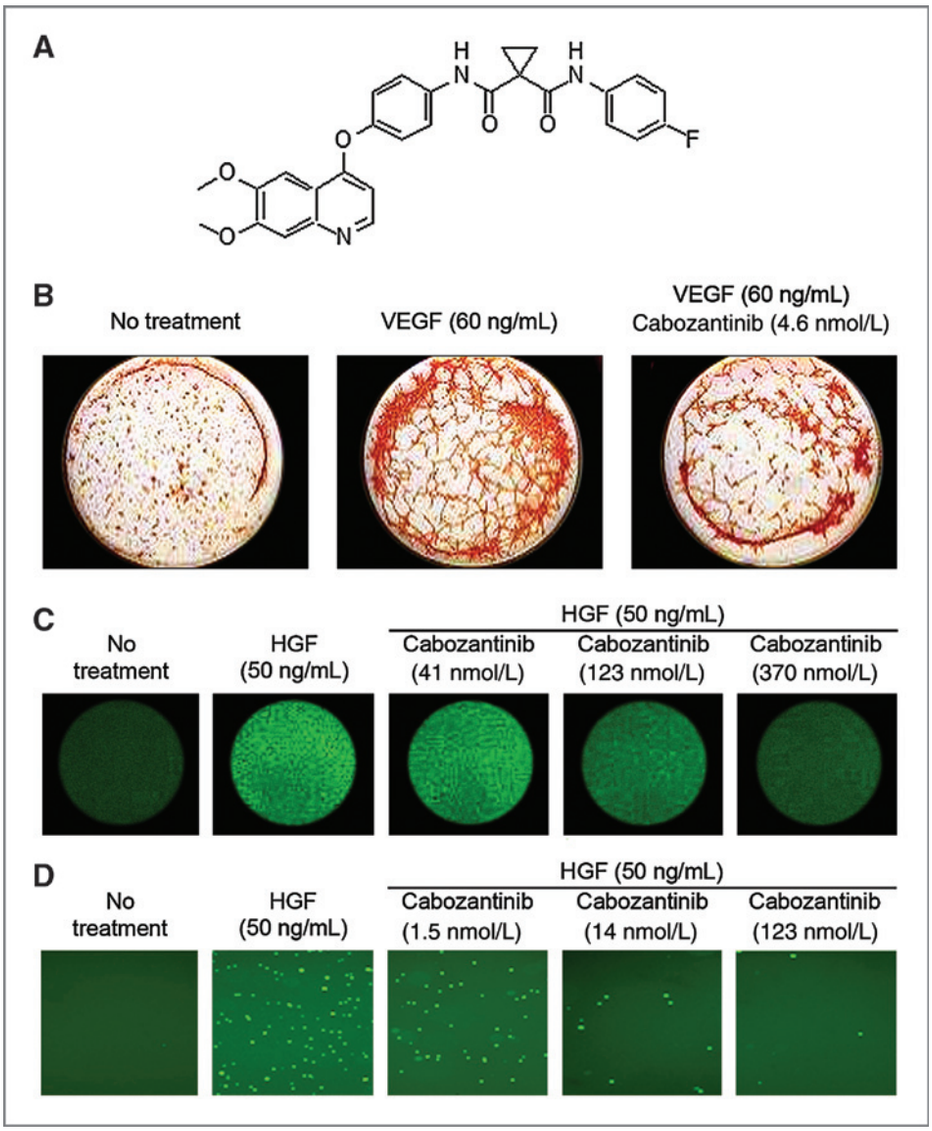

Figure 1. Cabozantinib inhibits VEGF-induced tubule formation and HGF-stimulated migration and invasion. A, chemical structure of cabozantinib. B, HMVEC-L cells were cocultured with human diploid fibroblasts for 7 days in the presence of VEGF (60 ng/mL) and cabozantinib, and tubule formation relative to VEGF-treated cells determined by immunostaining for the endothelial marker CD31. A representative image approximating the cabozantinib dose-response IC_{50} is shown (4.6 nmol/L). C, B16F10 cells were seeded in the upper chambers of a 96-well Transwell plate and incubated with cabozantinib, whereas the corresponding lower chambers contained HGF (50 ng/mL) and cabozantinib. Inhibition of migration was determined 24 hours later. D, B16F10 cells were seeded in the upper chambers of a 96-well Transwell plate coated with Matrigel and incubated with cabozantinib, whereas the corresponding lower chambers contained HGF (50 ng/mL) and cabozantinib. Inhibition of invasion was determined 24 hours later.

recovered from the lower chamber using Accutase (Innovative Cell Technologies). Cell suspensions were incubated with calcein AM (Molecular Probes; Invitrogen) and digital images captured with a fluorescence microscope. MS1 mouse endothelial cells were plated in 96-well plates coated with fibronectin. A cell-free zone was created that was followed by treatment with serially diluted cabozantinib and 30 ng/mL VEGF or 30 ng/mL HGF. After 20 hours, cell migration was determined from digitally captured images.

Cellular proliferation

Cells were seeded in triplicate overnight in media containing 10% FBS. The next day, cells were treated with serial dilutions of cabozantinib for 48 hours, followed by analysis of proliferation using Cell Proliferation ELISA, BrdUrd (Roche Applied Science).

In vivo inhibition of receptor phosphorylation

Female *nu/nu* mice (Taconic) were housed according to the Exelixis Institutional Animal Care and Use Committee guidelines. H441 cells (3×10^6) were implanted intradermally into the hind flank and when tumors reached approximately 150 mg, tumor weight was calculated using the formula: (tumor volume = length (mm) × width^2 (mm^2)]/2, mice were randomized ($n = 5$ per group) and orally administered a single 100 mg/kg dose of cabozantinib or vehicle. Tumors were collected at the indicated time points. Pooled tumor lysates were subjected to immunoprecipitation with anti-MET (SC161; Santa Cruz Biotechnology) and Western blotting with anti-phosphotyrosine MET (pY1230/34/35; BioSource International). After blot stripping, total MET was quantitated as a loading control. In a separate experiment, naive mice ($n = 5$ per group) were administered a single

Published OnlineFirst September 16, 2011; DOI: 10.1158/1535-7163.MCT-11-0264

100 mg/kg dose of cabozantinib or vehicle, followed by intravenous administration of HGF (10 μg per mouse) 10 minutes before liver collection. Analysis of MET phosphorylation in liver lysates was as described above. In a separate experiment, naive mice ($n = 5$ per group) were administered a single 100 mg/kg dose of cabozantinib or vehicle, followed by intravenous administration of VEGF (10 μg per mouse) 30 minutes before lung collection. Pooled lung lysates were subjected to immunoprecipitation with FLK1 (SC6251; Santa Cruz Biotechnology) and Western blotting with anti-phosphotyrosine (4G10, Upstate Biotechnology). After blot stripping, total FLK1 was quantitated as a loading control.

Immunohistochemistry

MDA-MB-231 cells (1×10^6) were implanted subcutaneously into the uncleared mammary fat pad of *nu/nu* mice. When the tumors reached approximately 100 mg (12 days after implantation), mice were randomized ($n = 8$ per group) and orally administered cabozantinib (100 mg/kg) or saline vehicle once daily for 4 days. Body weights were collected daily. Four hours before tumor harvest, animals were injected intraperitoneally with 60 mg/kg pimonidazole to facilitate visualization of tumor hypoxia. Tumors were resected at 4 and 8 hours after the first dose and 4 hours after the second, third, and fourth doses, respectively, snap frozen in optimum cutting temperature (Miles, Inc.) and processed for staining for hypoxia (Hypoxyprobe-1; Chemicon), vascularity [endothelial cell marker MECA-32 (#550563, BD Biosciences)], and proliferation [Ki67 (#RM-9106-S; Lab Vision)]. Apoptosis [terminal deoxynucleotidyl transferase–mediated dUTP nick end labeling (TUNEL)] determination was carried out using an In Situ Cell Death Detection Kit (Roche). Digital fluorescent images were captured using a Zeiss Axioskop 2 with AxioVision (Carl Zeiss MicroImaging LLC) image analysis software. One to 5 nonoverlapping representative fields were captured at ×5 (hypoxia, TUNEL, Ki67), ×100 (MECA-32), and ×400 (endothelial cell death) magnification and quantified using Metamorph (Molecular Devices).

Solid tumor efficacy studies

On day 0 in *nu/nu* mice, cells were inoculated intradermally into the hind flank (3×10^6 cells, H441) or subcutaneously into a noncleared mammary fat pad (1×10^6 cells, MBA-MB-231). When tumors reached approximately 100 mg (12–14 days after implantation), mice were randomized ($n = 10$ per group) and treated orally once daily for 14 days with cabozantinib or saline vehicle. In a separate study, MDA-MB-231 tumors were allowed to reach approximately 500 or 1,000 mg before randomization and initiation of cabozantinib treatment. On day 0 in female Wistar rats (Charles River Laboratories), C6 cells (5×10^6) were inoculated subcutaneously into the hind flank. When the tumors reached approximately 250 mg (3–4 days postimplantation), rats were randomized ($n = 8$ per group) and treated orally once daily for 12 days with cabozantinib or water vehicle. Body weights were collected daily, and tumor weights were collected twice weekly. Percentage of tumor growth inhibition/regression values were expressed as follows: 1 − [(mean treated tumor weight on the final day − mean tumor weight on day 0)/(mean vehicle tumor weight on the final day − mean tumor weight on day 0)] × 100. Statistical analysis of cabozantinib-treated tumors versus vehicle-treated tumors or versus predose tumors was done by one-way ANOVA with significance defined as $P < 0.05$. Blood was collected 4 hours after the final dose, and plasma was prepared to determine cabozantinib concentrations.

Experimental metastasis

On day 1, MDA-MB-231 cells (1×10^6) were implanted via tail vein injection into *nu/nu* mice that was immediately followed by randomization ($n = 12$–15 per group) and oral treatment with cabozantinib (60 mg/kg), sunitinib (120 mg/kg), or vehicle for 28 days. On day 28, lungs were perfused *in situ* with India ink solution (15% in PBS), resected, and lung wet weights immediately captured. Lungs were destained and fixed in Fekete's buffer (70% ethanol, 4% formaldehyde, glacial acetic acid; 20:2:1) for 72 hours, then transferred to 70% ethanol until image acquisition and analysis as previously described (23). Briefly, each lung was separated into 5 lobes, and ventral and dorsal surface aspects were digitally captured with lobes submerged under water. Images were analyzed by Definiens Developer XD to assess lung tumor foci counts. The number of tumor foci for ventral and dorsal lung surface aspects were obtained after applying size threshold parameters to exclude foci with diameters below 4 pixels from analysis (23). As the tumor foci data did not pass the normality and Gaussian distribution tests, statistical analysis was conducted via nonparametric ANOVA (Kruskal–Wallis analysis).

Results

Cabozantinib inhibits kinase activity

The selectivity of cabozantinib (Fig. 1A) was profiled against a protein kinase panel of approximately 270 human kinases. Cabozantinib is a potent inhibitor of MET and VEGFR2 with IC_{50} values of 1.3 and 0.035 nmol/L, respectively (Table 1). MET-activating kinase domain mutations Y1248H, D1246N, or K1262R were also inhibited by cabozantinib ($IC_{50} = 3.8$, 11.8, and 14.6 nmol/L, respectively). Cabozantinib displayed strong inhibition of several kinases that have also been implicated in tumor pathobiology, including KIT, RET, AXL, TIE2, and FLT3 ($IC_{50} = 4.6$, 5.2, 7, 14.3, and 11.3 nmol/L, respectively). Kinases not potently inhibited include RON, EGFR, IGFR1, and EphA4/B4. In cellular assays, cabozantinib inhibited phosphorylation of MET and VEGFR2, as well as KIT, FLT3, and AXL with IC_{50} values of 7.8, 1.9, 5.0, 7.5, and 42 μmol/L, respectively.

IC_{50} determinations conducted at various concentrations of ATP revealed that cabozantinib is an

Published OnlineFirst September 16, 2011; DOI: 10.1158/1535-7163.MCT-11-0264

Table 1. *In vitro* kinase inhibition profile of cabozantinib

Kinase	$IC_{50} \pm SD$,[a] nmol/L	Enzyme concentration, nmol/L	ATP concentration, μmol/L	Assay
VEGFR2	0.035 ± 0.01	0.05	3	A
MET	1.3 ± 1.2	10	1	C
MET (Y1248H)	3.8	13	1	C
MET (D1246N)	11.8	12	1	C
MET (K1262R)	14.6	12	1	C
RET	5.2 ± 4.3	15	2	C
TIE2	14.3 ± 1.1	15	5	R
AXL	7	TBD	TBD	TBD
FLT3	11.3 ± 1.8	0.5	1	C
KIT	4.6 ± 0.5	1	3	A
RON	124 ± 1.2	60	1	C

Abbreviations: A, AlphaScreen; C, Coupled luciferase; R, radiometric; TBD, to be determined.
[a]Mean ± SD of at least 3 independent determinations.

ATP-competitive inhibitor of MET, VEGFR2, TIE2, and FLT3 (data not shown). Kinetic constants for binding to MET and VEGFR2 show tight but reversible binding (Supplementary Table S1).

Cabozantinib inhibits endothelial cell tubule formation *in vitro*

HMVEC cells were incubated with VEGF in the presence of cabozantinib and tubule formation visualized by immunostaining for CD31. Cabozantinib inhibited tubule formation with an IC_{50} value of 6.7 nmol/L (Fig. 1B) with no evidence of cytotoxicity, showing that cabozantinib exerts an antiangiogenic rather than cytotoxic effect. Cabozantinib also inhibited tubule formation in response to conditioned media derived from cultures of MDA-MB-231 (IC_{50} = 5.1 nmol/L), A431 (IC_{50} = 4.1 nmol/L), HT1080 (IC_{50} = 7.7 nmol/L), and B16F10 (IC_{50} = 4.7 nmol/L) cells, suggesting that secreted tumor cell–derived proangiogenic growth factors are unable to circumvent inhibition of tubule formation by cabozantinib.

Cabozantinib inhibits cellular migration and invasion

We have previously shown that HGF promotes MET phosphorylation in B16F10 cells and stimulates migration and invasion (24). Cabozantinib potently inhibited HGF-induced migration (IC_{50} = 31 nmol/L; Fig. 1C) and invasion (IC_{50} = 9 nmol/L; Fig. 1D) of B16F10 cells. VEGF- and HGF-mediated migration of proangiogenic murine MS1 endothelial cells (25) were also sensitive to cabozantinib with IC_{50} values of 5.8 and 41 nmol/L, respectively.

Cabozantinib inhibits tumor cell proliferation in a variety of tumor types

The effect of cabozantinib on proliferation was evaluated in a number of human tumor cell lines. SNU-5 and Hs746T cells harboring amplified MET (26) were the most sensitive to cabozantinib (IC_{50} = 19 and 9.9 nmol/L, respectively); however, SNU-1 and SNU-16 cells lacking MET amplification were more resistant (IC_{50} = 5,223 and 1,149 nmol/L, respectively). MDA-MB-231 and U87MG cells exhibited comparable levels of sensitivity to cabozantinib (IC_{50} = 6,421 and 1,851 nmol/L, respectively), whereas H441, H69, and PC3 cell lines were the least sensitive to cabozantinib with IC_{50} values of 21,700, 20,200, and 10,800 nmol/L, respectively. In addition, BaF3 cells expressing human FLT3-ITD, an activating mutation in acute myelogenous leukemia (27), were sensitive to cabozantinib (IC_{50} = 15 nmol/L) when compared with wild-type BaF3 cells (IC_{50} = 9,641 nmol/L).

Cabozantinib inhibits MET and VEGFR2 phosphorylation *in vivo*

A single 100 mg/kg oral dose of cabozantinib resulted in inhibition of phosphorylation of MET 2 to 8 hours postdose in H441 tumors that harbor constitutively phosphorylated MET (Fig. 2A). This result is consistent with data showing the sensitivity of these cells to inhibitors selective for MET and MET knockdown by siRNA (28, 29). This effect was reversible, as MET phosphorylation returned to basal levels by 48 hours after treatment. In separate experiments, cabozantinib inhibited *in vivo* stimulation of MET phosphorylation by HGF in liver hepatocytes (Fig. 2B) and VEGF-stimulated phosphorylation of FLK1 (Fig. 2C) with inhibition of both targets sustained through 8 hours postdose. Furthermore, cabozantinib eliminated endogenous levels of phosphorylated FLK1 that are present in the absence of VEGF stimulation. Plasma concentrations of cabozantinib (Supplementary Table S2) associated with maximal and sustained inhibition of MET and FLK1 were 17 to 34 μmol/L, greater than 3-fold above the MET cellular phosphorylation, VEGF tubule formation, and HGF invasion IC_{50} values described above.

Published OnlineFirst September 16, 2011; DOI: 10.1158/1535-7163.MCT-11-0264

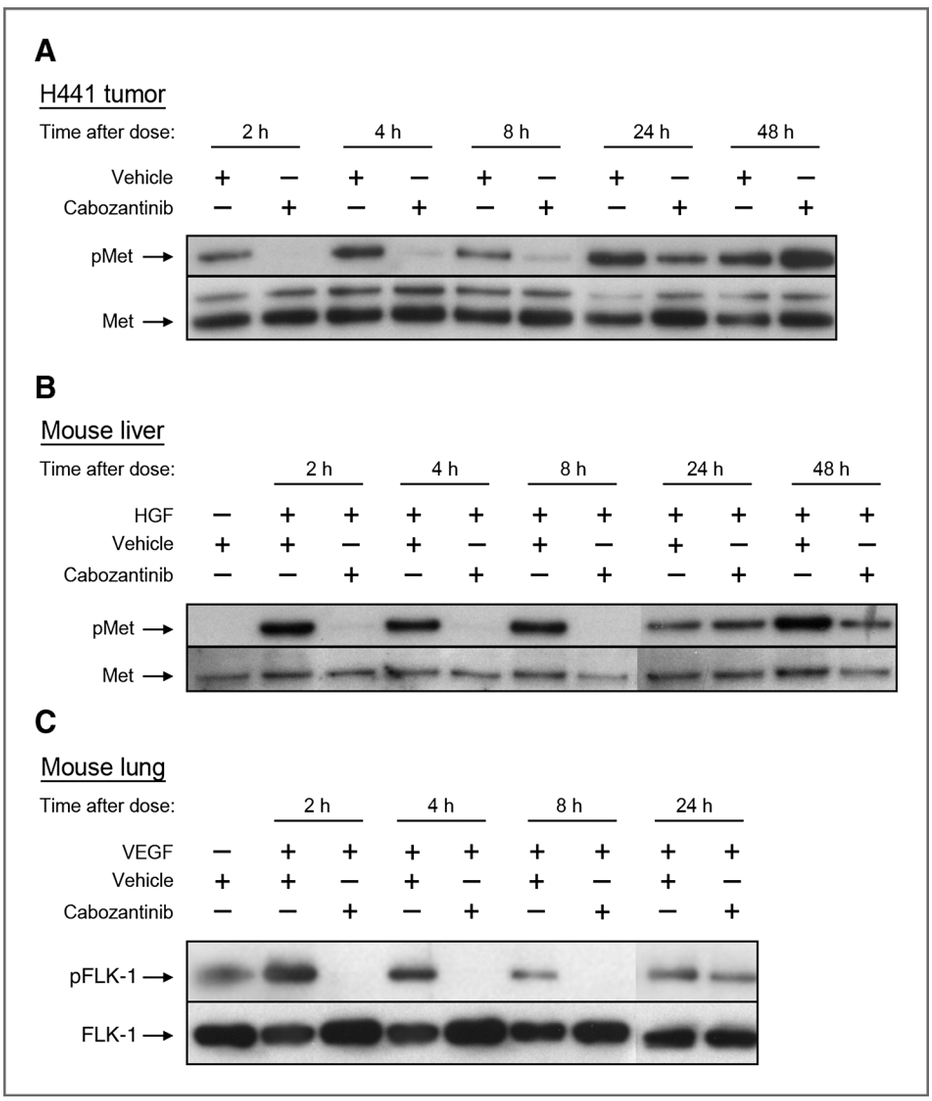

Figure 2. Cabozantinib treatment results in inhibition of phosphorylation of MET in tumor and liver tissue and phosphorylation of FLK1 in lung tissue following a single oral dose. A, mice bearing H441 tumors were administered a single oral dose of cabozantinib (100 mg/kg) or water vehicle, and levels of phosphorylated and total MET in tumor lysates were determined. B, naive mice were administered a single dose of cabozantinib (100 mg/kg) or water vehicle. Ten minutes before harvest, mice were intravenously administered HGF (10 μg per animal), and levels of phosphorylated and total MET in liver lysates were determined. C, naive mice were administered a single dose of cabozantinib (100 mg/kg) or water vehicle. Thirty minutes before harvest, mice were intravenously administered VEGF (10 μg per animal), and levels of phosphorylated and total FLK1 in lung lysates were determined. Representative Western blot images are shown.

Cabozantinib disrupts tumor vasculature and promotes tumor and endothelial cell death

To examine the effect of cabozantinib on tumor vasculature, antiangiogenic-sensitive MDA-MB-231 cells expressing MET and VEGF were used (28, 30). Tumor-bearing animals were administered a 100-mg/kg oral dose, and tumors were collected 4 and 8 hours after the first dose and 4 hours after the consecutive second, third, and fourth doses. Vehicle-treated tumors exhibited low levels of hypoxia ($\leq$1%) and TUNEL ($\leq$0.5%), and high levels of Ki67 ($\geq$60%) and MECA-32 ($\geq$20%), indicative of viable, highly proliferative, and vascularized tumors (data not shown). Cabozantinib significantly increased tumor hypoxia (13-fold; Fig. 3A) and apoptosis (TUNEL; 2.5-fold; Fig. 3B) at 8 and 4 hours after the first and second doses, respectively, when compared with vehicle-treated tumors collected at the same time point. Concomitant reductions in the proliferation marker Ki67 (19%; Fig. 3C) and the endothelial cell surface marker MECA-32 (12%; Fig. 3D) were also observed 8 hours after a single dose. Progressive, marked changes in these endpoints continued such that after the third dose, the number of apoptotic and hypoxic cells were elevated 78- and 85-fold, respectively, whereas marked reductions in Ki67 (55%) and MECA-32 (75%) were also evident. Summarized quantitative data are provided in Supplementary Table S3. Despite these profound and progressive effects of cabozantinib on tumor physiology, animals seemed healthy with no visible signs of toxicity or loss of body weight (data not shown).

The rapid decrease of MECA-32 prompted closer examination of tumor endothelial cell survival. Simultaneous examination of TUNEL-, MECA-32-, and 4′,6-diamidino-2-phenylindole–stained cells revealed cabozantinib-induced cell death not only in tumor cells but also in endothelial cells in the tumor vasculature (Fig. 3E). Taken

Published OnlineFirst September 16, 2011; DOI: 10.1158/1535-7163.MCT-11-0264

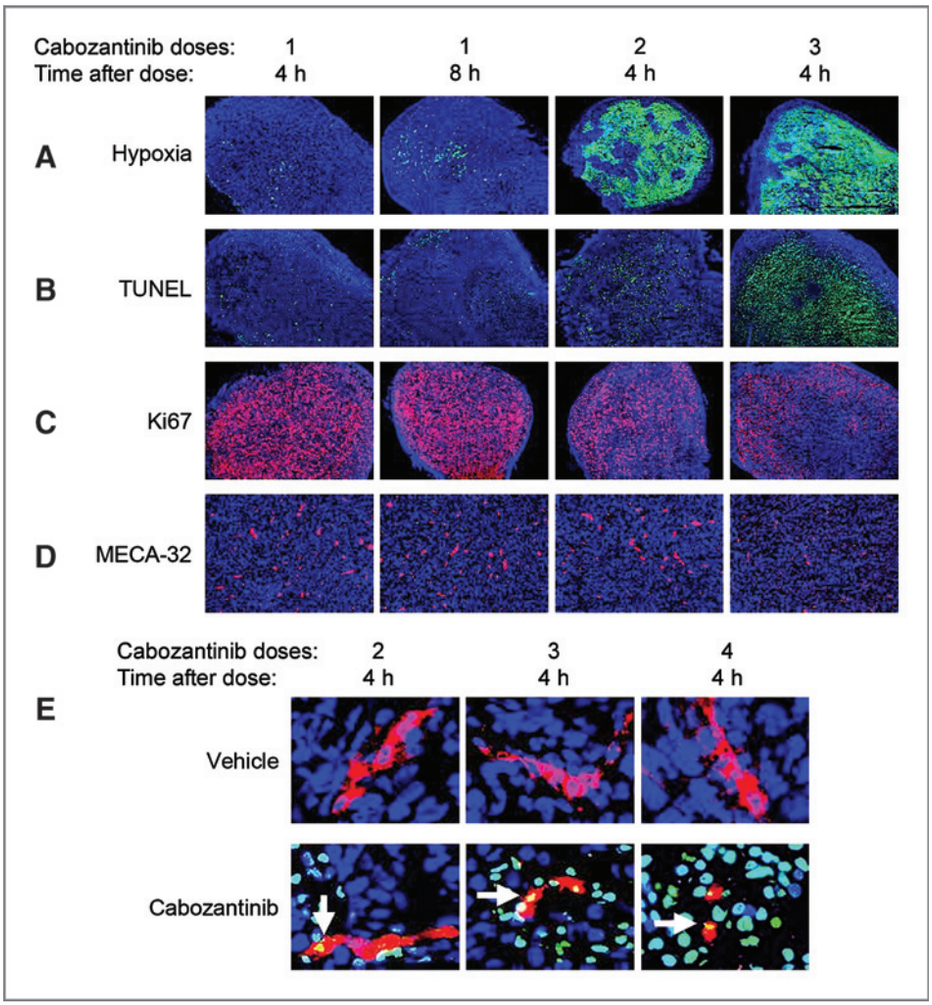

Figure 3. Cabozantinib causes rapid increases in tumor hypoxia (A) and cell death (B) and decreases in proliferation (C) and vascularity (D) in MDA-MB-231 tumors. MDA-MB-231 tumor-bearing mice were orally administered cabozantinib (100 mg/kg) or vehicle once daily for 4 days. Tumors were resected 4 and 8 hours after the first dose and 4 hours after the second, third, and fourth doses and processed for immunofluorescence evaluation of tumor hypoxia, apoptosis (TUNEL), proliferation (Ki67), and tumor vascularity (MECA-32). Digital images were captured at ×5 (hypoxia, TUNEL, and Ki67) and ×100 (MECA-32) magnifications. E, additional tumor sections were processed for simultaneous evaluation of viable tumor cells (blue), tumor endothelial cells (red), and cell death (green). Arrows indicate regions of endothelial cell death (yellow color resulting from red and green overlay). Digital images were captured at ×400 magnification.

together, these results show that cabozantinib disrupts tumor vasculature by inducing endothelial cell death that negatively impacts tumor viability.

Cabozantinib inhibits tumor growth in a dose-dependent manner

The *in vivo* efficacy of cabozantinib was evaluated in human tumor models in rodents over a period of time that corresponded to exponential tumor growth of each model. Cabozantinib treatment resulted in significant tumor growth inhibition of MDA-MB-231 tumors ($P < 0.001$) for all doses when compared with vehicle-treated tumors (Fig. 4A). Dose-dependent inhibition was observed for the 3- and 10-mg/kg doses ($P < 0.01$). At the 30- and 60-mg/kg doses, cabozantinib induced stable disease. Continuous treatment at these doses was associated with plasma concentrations of 9,000 to 16,000 nmol/L, which was ~2-fold above IC_{50} values for cellular proliferation and tubule formation with MDA-MB-231 conditioned media. A single 100 mg/kg dose resulted in sustained MDA-MB-231 tumor growth inhibition for approximately 8 days after which tumors began growing at a rate similar to vehicle-treated control tumors (Supplementary Fig. S1A). In a similar but separate study with larger MDA-MB-231 tumors, a 10-mg/kg dose resulted in induction of stable disease that was independent of initial tumor size (Fig. 4B), whereas a 60-mg/kg dose resulted in significant tumor regression of both 500-mg (37%, $P = 0.0003$) and 1,000-mg (45%, $P = 0.0001$) tumors. Cabozantinib inhibited growth of H441 tumors at all doses ($P < 0.001$), with dose-dependent inhibition observed for the 10- and 30-mg/kg doses (Fig. 4C). The 60-mg/kg dose resulted in significant tumor regression (33%, $P < 0.005$) when compared with predose tumor weights. As elevated MET expression has been detected in human gliomas and implicated in glioma cell growth (29, 31), the antitumor effect of cabozantinib in the MET-expressing rat C6 glioma cell line (32) was determined. Cabozantinib inhibited tumor growth ($P < 0.001$) for all doses when compared with vehicle-treated tumors (Fig. 4D). Moreover, the 3- and 10-mg/kg doses resulted in significant tumor regression (62 and 85%, $P < 0.0001$) when compared with predose tumor weights. In a separate experiment, a single 10-mg/kg dose resulted in C6 tumor growth inhibition

Published OnlineFirst September 16, 2011; DOI: 10.1158/1535-7163.MCT-11-0264

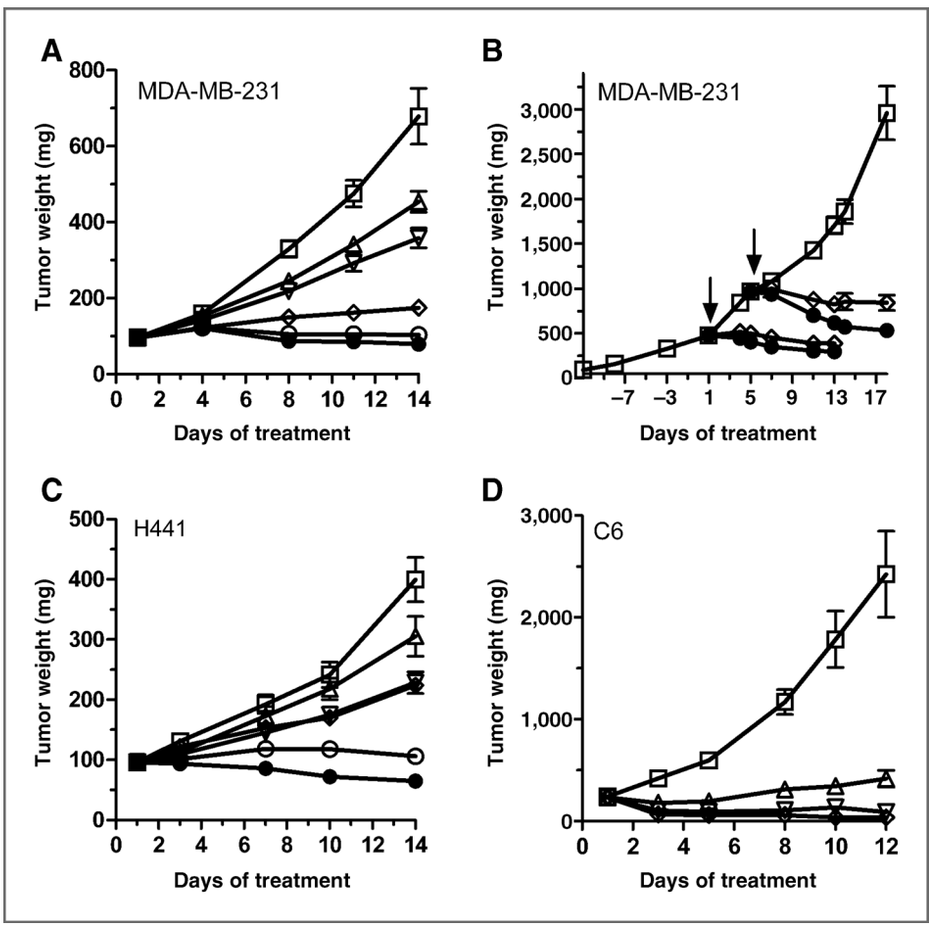

Figure 4. Cabozantinib inhibits tumor growth and promotes tumor regression. Animals bearing established MDA-MB-231 (A and B), H441 (C), and C6 (D) tumors were orally administered once daily vehicle (□) or cabozantinib at 1 mg/kg (Δ), 3 mg/kg (▽), 10 mg/kg (■), 30 mg/kg (○), or 60 mg/kg (●) for 12 to 14 days, depending on the model. Tumor weights were determined twice weekly. Data points represent the mean tumor weight (in milligrams) and SE for each treatment group. Arrows in B represent onset of cabozantinib treatment.

that was sustained during a 15-day observation period (Supplementary Fig. S1B). On a body weight dosage basis, cabozantinib plasma exposures ranged from 6- to 10-fold higher in rats than in mice (Supplementary Table S4), which accounts for lower doses inducing tumor growth inhibition/regression in rats than in mice. Subchronic administration of cabozantinib was well tolerated in mice and rats with no signs of toxicity, as determined by stable and/or increasing body weights during the treatment period (Supplementary Fig. S1C and S1D).

Cabozantinib does not promote metastasis following intravenous tumor cell inoculation

The impact of cabozantinib on metastasis to that of VEGFR2-targeting therapies, known to promote metastasis in preclinical models (17), was investigated. Immediately following intravenous injection of MDA-MB-231 cells into mice, oral cabozantinib or sunitinib treatment was initiated and continued once daily for 28 days. Examination of intact lungs from cabozantinib-treated mice revealed no apparent difference in lung surface tumor burden when compared with lungs from vehicle-treated control animals (Fig. 5A); however, lungs from sunitinib-treated animals displayed an apparent increase in tumor burden. Quantitation of tumor foci per lobe surface revealed no statistical difference in the number of foci for vehicle- and cabozantinib-treated mice (56 vs. 64 foci/lobe surface, $P > 0.05$) and a 2-fold increase in tumor foci for sunitinib-treated mice (109 foci/lobe surface, $P < 0.001$; Fig. 5B). Additional evidence of inhibition of metastasis was confirmed by lack of a significant increase ($P > 0.05$) in whole lung wet weights in cabozantinib-treated animals (Fig. 5C). Cabozantinib treatment was well tolerated as determined by stable body weights throughout the 28-day treatment period.

Discussion

The MET signaling pathway has been shown to be important in tumor growth, survival, and metastasis and acts synergistically with VEGF to promote angiogenesis (8, 9). Both MET and VEGF are found to be dysregulated in many tumor types, resulting in tumor angiogenesis and tumor cell proliferation and invasion. Because of the synergistic effects of MET and VEGFR signaling, inhibiting both arms of the MET/VEGF axis may offer significant benefit over targeting either pathway individually.

Published OnlineFirst September 16, 2011; DOI: 10.1158/1535-7163.MCT-11-0264

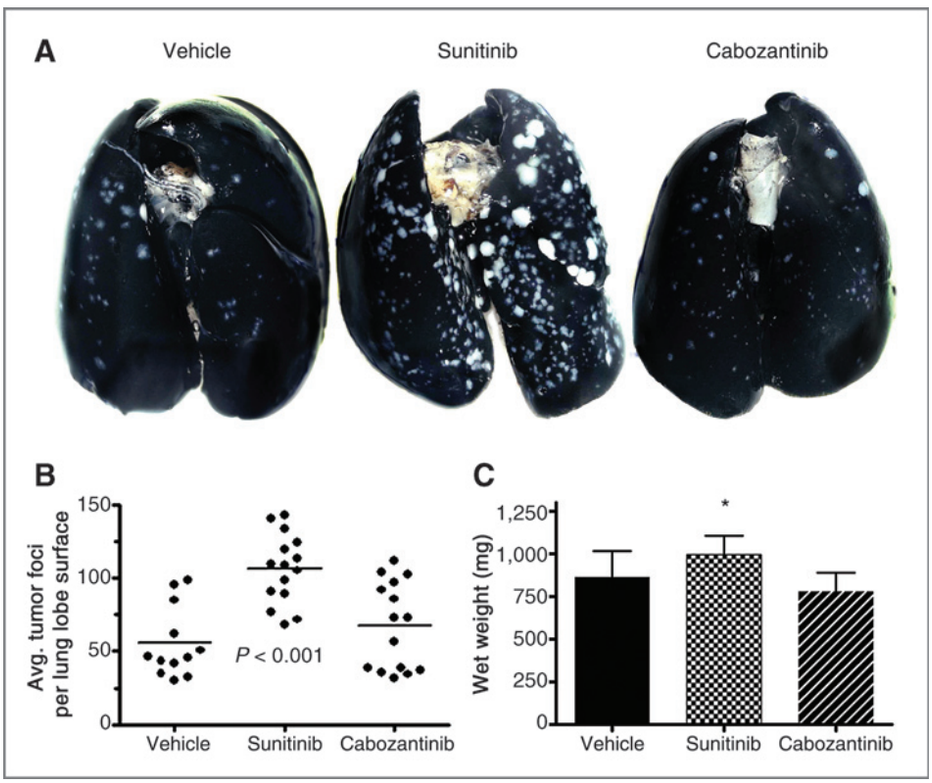

Figure 5. Treatment with cabozantinib does not accelerate tumor growth in an experimental model of metastasis. On day 1, MDA-MB-231 cells (1×10^6) were injected intravenously into the tail vein of female mice, which was immediately followed by daily oral administration of vehicle, cabozantinib (60 mg/kg), or sunitinib (120 mg/kg) for 28 days. A, representative images showing surface tumor foci from the indicated treatment groups on day 28 posttumor cell implantation. B, scatter plot depicting the number of tumor foci following 28 days of cabozantinib, sunitinib, or vehicle treatment. The number of tumor foci in cabozantinib-treated lungs was not significantly different when compared with the number of tumor foci in vehicle-treated lungs ($P > 0.05$). C, whole lung wet weights on day 28 posttumor cell implantation. *, $P < 0.001$.

In tumor cells, inappropriate activation of MET occurs through overexpression of wild-type MET or its ligand HGF or as a result of activating mutations in the gene encoding MET. Importantly, cabozantinib potently inhibits both wild-type MET and MET with activating mutations, such as those frequently found in hereditary papillary renal and hepatocellular carcinomas (33, 34). Further evidence for the potent activity of cabozantinib comes from cell proliferation studies, where it robustly inhibited cell lines known to be dependent on MET but not cell lines known to be independent of MET.

As shown in this report, cabozantinib exhibits potent and reversible inhibition of its targets, leading to disruption of cellular processes that have been implicated in angiogenesis and tumorigenesis, including migration and tubule formation. This translates into profound changes in tumor physiology, including widespread endothelial and tumor cell apoptosis, disruptions in tumor vasculature, and increased hypoxia. Subchronic treatment with cabozantinib results in broad antitumor efficacy, and in some models, tumor regression; however, a single dose exhibits antitumor efficacy for approximately 8 to 15 days in the models examined.

We used a variety of tumor models that are driven by diverse mechanisms. H441 cells overexpress constitutively active MET as well as activated EGFR, HER2, and HER3 (35). C6 rat glioma cells overexpress MET and are PTEN deficient (32, 36). While MDA-MB-231 cells do not overexpress MET, they are responsive to HGF and also harbor mutationally activated forms of RAS and RAF (37, 38). None of these cell lines are known to be strictly addicted to or dependent on signaling through MET for proliferation, consistent with their relative resistance to cabozantinib *in vitro*. However, our studies with cabozantinib suggest that the observed antitumor efficacy is the result of mechanisms affecting tumor angiogenesis and the blockade of invasive tumor growth rather than the result of directly targeting cellular proliferation.

One of the limitations of VEGF-targeted therapies has been a lack of enduring clinical benefit. Bergers and Hanahan recently theorized that tumor cells may develop resistance to antiangiogenic therapies through adaptive mechanisms such as upregulation of alternative proangiogenic signaling pathways and enhancement of metastasis (39). Indeed, VEGFR inhibitors such as sunitinib, sorafenib, cediranib, VEGFR2-targeting antibodies, and neutralizing antimurine VEGF antibodies have all been observed to increase the invasiveness and/or metastatic potential of tumors (17, 18, 19, 40). Ebos and colleagues hypothesized that treatment with sunitinib may lead to upregulation of cytokines that promote metastasis (17), and recent studies have suggested that the MET/HGF pathway is important for proangiogenic and prometastatic signaling in the context of VEGF inhibition (16, 19, 40). In light of these observations, it is interesting that our results show that cabozantinib produces potent antitumor and antiangiogenic effects without increasing tumor metastatic potential, unlike treatment with sunitinib, suggesting that targeting MET and VEGFR2 simultaneously may cut off metastatic escape pathways. A

Published OnlineFirst September 16, 2011; DOI: 10.1158/1535-7163.MCT-11-0264

recent study using RIP-Tag2 transgenic mice similarly showed that treatment with cabozantinib resulted in more extensive tumor shrinkage and decreased tumor invasiveness and metastasis than treatment with vehicle or anti-VEGF antibody. Strikingly, in that study, all of the mice treated with cabozantinib survived until the experiment ended at 20 weeks, whereas none of the vehicle- or anti-VEGF antibody–treated mice survived to that endpoint (40). Together, these data suggest that inhibiting MET and VEGFR2 with cabozantinib effectively blocks the development of MET-driven evasive resistance seen with agents targeting the VEGF pathway alone, thereby providing a more sustained antitumor effect.

Our results provide support for testing cabozantinib in a broad variety of tumors where MET activation has been implicated and/or VEGF pathway inhibitors have shown efficacy. Cabozantinib is currently being studied in clinical trials in a number of tumor types, including medullary and differentiated thyroid, prostate, ovarian, non–small cell lung, hepatocellular, renal cell, and breast cancers, as well as melanoma and glioblastoma (41). In clinical trials, cabozantinib was generally well tolerated, with promising clinical activity and response in multiple tumor types (42–49). The data presented here show that cabozantinib has potent antimetastatic, antitumor, and antiangiogenic activity in preclinical models, and they support the ongoing evaluation of the clinical activity of cabozantinib in patients with a variety of cancers.

Disclosure of Potential Conflicts of Interest

All authors are employees of Exelixis, Inc.

Acknowledgments

The authors thank Dana Aftab and Peter Lamb for critical reading of the manuscript, Barbara Sennino for assistance with the migration images, and Cheryl Chun of BlueMomentum.

Grant Support

The financial support was provided by Exelixis, Inc. The funding for BlueMomentum was provided by Exelixis.

The costs of publication of this article were defrayed in part by the payment of page charges. This article must therefore be hereby marked *advertisement* in accordance with 18 U.S.C. Section 1734 solely to indicate this fact.

Received April 7, 2011; revised September 9, 2011; accepted September 13, 2011; published OnlineFirst September 16, 2011.

References

1. Birchmeier C, Birchmeier W, Gherardi E, Vande Woude GF. Met, metastasis, motility and more. Nat Rev Mol Cell Biol 2003;4:915–25.
2. Rong S, Segal S, Anver M, Resau JH, Vande Woude GF. Invasiveness and metastasis of NIH 3T3 cells induced by Met-hepatocyte growth factor/scatter factor autocrine stimulation. Proc Natl Acad Sci U S A 1994;91:4731–5.
3. Michieli P, Mazzone M, Basilico C, Cavassa S, Sottile A, Naldini L, et al. Targeting the tumor and its microenvironment by a dual-function decoy Met receptor. Cancer Cell 2004;6:61–73.
4. Boccaccio C, Sabatino G, Medico E, Girolami F, Follenzi A, Reato G, et al. The MET oncogene drives a genetic programme linking cancer to haemostasis. Nature 2005;434:396–400.
5. Takayama H, LaRochelle WJ, Sharp R, Otsuka T, Kriebel P, Anver M, et al. Diverse tumorigenesis associated with aberrant development in mice overexpressing hepatocyte growth factor/scatter factor. Proc Natl Acad Sci U S A 1997;94:701–6.
6. Abounader R, Lal B, Luddy C, Koe G, Davidson B, Rosen EM, et al. *In vivo* targeting of SF/HGF and c-met expression via U1snRNA/ribozymes inhibits glioma growth and angiogenesis and promotes apoptosis. FASEB J 2002;16:108–10.
7. Christensen JG, Burrows J, Salgia R. c-Met as a target for human cancer and characterization of inhibitors for therapeutic intervention. Cancer Lett 2005;225:1–26.
8. Xin X, Yang S, Ingle G, Zlot C, Rangell L, Kowalski J, et al. Hepatocyte growth factor enhances vascular endothelial growth factor-induced angiogenesis *in vitro* and *in vivo*. Am J Pathol 2001;158:1111–20.
9. Van Belle E, Witzenbichler B, Chen D, Silver M, Chang L, Schwall R, et al. Potentiated angiogenic effect of scatter factor/hepatocyte growth factor via induction of vascular endothelial growth factor: the case for paracrine amplification of angiogenesis. Circulation 1998;97:381–90.
10. Hurwitz H, Fehrenbacher L, Novotny W, Cartwright T, Hainsworth J, Heim W, et al. Bevacizumab plus irinotecan, fluorouracil, and leucovorin for metastatic colorectal cancer. N Engl J Med 2004;350:2335–42.
11. Motzer RJ, Hutson TE, Tomczak P, Michaelson MD, Bukowski RM, Oudard S, et al. Overall survival and updated results for sunitinib compared with interferon alfa in patients with metastatic renal cell carcinoma. J Clin Oncol 2009;27:3584–90.
12. Escudier B, Eisen T, Stadler WM, Szczylik C, Oudard S, Siebels M, et al. Sorafenib in advanced clear-cell renal-cell carcinoma. N Engl J Med 2007;356:125–34.
13. Casanovas O, Hicklin DJ, Bergers G, Hanahan D. Drug resistance by evasion of antiangiogenic targeting of VEGF signaling in late-stage pancreatic islet tumors. Cancer Cell 2005;8:299–309.
14. Kitajima Y, Ide T, Ohtsuka T, Miyazaki K. Induction of hepatocyte growth factor activator gene expression under hypoxia activates the hepatocyte growth factor/c-Met system via hypoxia inducible factor-1 in pancreatic cancer. Cancer Sci 2008;99:1341–7.
15. Pennacchietti S, Michieli P, Galluzzo M, Mazzone M, Giordano S, Comoglio PM. Hypoxia promotes invasive growth by transcriptional activation of the met protooncogene. Cancer Cell 2003;3:347–61.
16. Shojaei F, Lee JH, Simmons BH, Wong A, Esparza CO, Plumlee PA, et al. HGF/c-Met acts as an alternative angiogenic pathway in sunitinib-resistant tumors. Cancer Res 2010;70:10090–100.
17. Ebos JM, Lee CR, Cruz-Munoz W, Bjarnason GA, Christensen JG, Kerbel RS. Accelerated metastasis after short-term treatment with a potent inhibitor of tumor angiogenesis. Cancer Cell 2009;15:232–9.
18. Pàez-Ribes M, Allen E, Hudock J, Takeda T, Okuyama H, Viñals F, et al. Antiangiogenic therapy elicits malignant progression of tumors to increased local invasion and distant metastasis. Cancer Cell 2009;15:220–31.
19. di Tomaso E, Snuderl M, Kamoun WS, Duda DG, Auluck PK, Fazlollahi L, et al. Glioblastoma recurrence after cediranib therapy in patients: lack of "rebound" revascularization as mode of escape. Cancer Res 2011;71:19–28.
20. Castellone MD, Carlomagno F, Salvatore G, Santoro M. Receptor tyrosine kinase inhibitors in thyroid cancer. Best Pract Res Clin Endocrinol Metab 2008;22:1023–38.
21. Tímár J, Döme B. Antiangiogenic drugs and tyrosine kinases. Anticancer Agents Med Chem 2008;8:462–9.
22. Bannen LC, Chan DS, Forsyth TP, Khoury RG, Leahy JW, Mac MB, et al. inventors; Exelixis, Inc., assignee. c-Met modulators and

Published OnlineFirst September 16, 2011; DOI: 10.1158/1535-7163.MCT-11-0264

methods of use. United States patent US 7579473. 2009Aug 25. [cited 2011 Aug 8]. Available from: http://patents.justia.com/2009/07579473.html.

23. Watts AM, Kennedy RC. Quantitation of tumor foci in an experimental murine model using computer-assisted video imaging. Anal Biochem 1998;256:217–19.
24. Qian F, Engst S, Yamaguchi K, Yu P, Won KA, Mock L, et al. Inhibition of tumor cell growth, invasion, and metastasis by EXEL-2880 (XL880, GSK1363089), a novel inhibitor of HGF and VEGF receptor tyrosine kinases. Cancer Res 2009;69:8009–16.
25. Arbiser JL, Moses MA, Fernandez CA, Ghiso N, Cao Y, Klauber N, et al. Oncogenic H-ras stimulates tumor angiogenesis by two distinct pathways. Proc Natl Acad Sci U S A 1997;94:861–6.
26. Smolen GA, Sordella R, Muir B, Mohapatra G, Barmettler A, Archibald H, et al. Amplification of MET may identify a subset of cancers with extreme sensitivity to the selective tyrosine kinase inhibitor PHA-665752. Proc Natl Acad Sci U S A 2006;103:2316–21.
27. Kottaridis PD, Gale RE, Frew ME, Harrison G, Langabeer SE, Belton AA, et al. The presence of a FLT3 internal tandem duplication in patients with acute myeloid leukemia (AML) adds important prognostic information to cytogenetic risk group and response to the first cycle of chemotherapy: analysis of 854 patients from the United Kingdom Medical Research Council AML 10 and 12 trials. Blood 2001;98:1752–9.
28. Munshi N, Jeay S, Li Y, Chen CR, France DS, Ashwell MA, et al. ARQ 197, a novel and selective inhibitor of the human c-Met receptor tyrosine kinase with antitumor activity. Mol Cancer Ther 2010;9:1544–53.
29. Christensen JG, Schreck R, Burrows J, Kuruganti P, Chan E, Le P, et al. A selective small molecule inhibitor of c-Met kinase inhibits c-Met-dependent phenotypes *in vitro* and exhibits cytoreductive antitumor activity *in vivo*. Cancer Res 2003;63:7345–55.
30. Roland CL, Dineen SP, Lynn KD, Sullivan LA, Dellinger MT, Sadegh L, et al. Inhibition of vascular endothelial growth factor reduces angiogenesis and modulates immune cell infiltration of orthotopic breast cancer xenografts. Mol Cancer Ther 2009;8:1761–71.
31. Chu S, Yuan X, Li Z, Jiang P, Zhang J. C-Met antisense oligodeoxynucleotide inhibits growth of glioma cells. Surg Neurol 2006;65:533–8.
32. Towner RA, Smith N, Doblas S, Tesiram Y, Garteiser P, Saunders D, et al. *In vivo* detection of c-Met expression in a rat C6 glioma model. J Cell Mol Med 2008;12:174–86.
33. Schmidt L, Junker K, Nakaigawa N, Kinjerski T, Weirich G, Miller M, et al. Novel mutations of the MET proto-oncogene in papillary renal carcinomas. Oncogene 1999;18:2343–50.
34. Park WS, Dong SM, Kim SY, Na EY, Shin MS, Pi JH, et al. Somatic mutations in the kinase domain of the Met/hepatocyte growth factor receptor gene in childhood hepatocellular carcinomas. Cancer Res 1999;59:307–10.
35. Agarwal S, Zerillo C, Kolmakova J, Christensen JG, Harris LN, Rimm DL, et al. Association of constitutively activated hepatocyte growth factor receptor (Met) with resistance to a dual EGFR/Her2 inhibitor in non-small-cell lung cancer cells. Br J Cancer 2009;100:941–9.
36. Kubiatowski T, Jang T, Lachyankar MB, Salmonsen R, Nabi RR, Quesenberry PJ, et al. Association of increased phosphatidylinositol 3-kinase signaling with increased invasiveness and gelatinase activity in malignant gliomas. J Neurosurg 2001;95:480–8.
37. Trusolino L, Cavassa S, Angelini P, Andó M, Bertotti A, Comoglio PM, et al. HGF/scatter factor selectively promotes cell invasion by increasing integrin avidity. FASEB J 2000;14:1629–40.
38. Hollestelle A, Elstrodt F, Nagel JH, Kallemeijn WW, Schutte M. Phosphatidylinositol-3-OH kinase or RAS pathway mutations in human breast cancer cell lines. Mol Cancer Res 2007;5:195–201.
39. Bergers G, Hanahan D. Modes of resistance to anti-angiogenic therapy. Nat Rev Cancer 2008;8:592–603.
40. Sennino B, Naylor RM, Tabruyn SP, You W-K, Aftab DT, McDonald DM. Reduction of tumor invasiveness and metastasis and prolongation of survival of RIP-Tag2 mice after inhibition of VEGFR plus c-Met by XL184. Mol Cancer Ther 2009;8(12 Suppl):A13.
41. Zhang Y, Guessous F, Kofman A, Schiff D, Abounader R. XL-184, a MET, VEGFR-2 and RET kinase inhibitor for the treatment of thyroid cancer, glioblastoma multiforme and NSCLC. IDrugs 2010;13:112–21.
42. Kurzrock R, Sherman SI, Ball DW, Forastiere AA, Cohen RB, Mehra R, et al. Activity of XL184 (cabozantinib), an oral tyrosine kinase inhibitor, in patients with medullary thyroid cancer. J Clin Oncol 2011;29:2660–6
43. Wen PY, Prados M, Schiff D, Reardon DA, Cloughesy T, Mikkelsen T, et al. Phase II study of XL184 (BMS 907351), an inhibitor of MET, VEGFR2, and RET, in patients (pts) with progressive glioblastoma (GB). J Clin Oncol 28:15s, 2010 (suppl; abstr 2006).
44. Gordon MS, Vogelzang NJ, Schoffski P, Daud A, Spira AI, O'Keeffe BA, et al. Activity of cabozantinib (XL184) in soft tissue and bone: results of a phase II randomized discontinuation trial (RDT) in patients (pts) with advanced solid tumors. J Clin Oncol 29:15s, 2011 (suppl; abstr 3010).
45. Nechushtan H, Edelman G, Jerusalem G, Gordon M, Kluger HM, Moussa A, et al. Phase 2 results of XL184 in a cohort of patients (pts) with advanced melanoma. Eur J Cancer 2010;8:7. Abstract 398.
46. Hussain M, Smith MR, Sweeney C, Corn PG, Elfiky A, Gordon MS, et al. Cabozantinib (XL184) in metastatic castration-resistant prostate cancer (mCRPC): results from a phase II randomized discontinuation trial. J Clin Oncol 29:15s, 2011 (suppl; abstr 4516).
47. Buckanovich RJ, Berger R, Sella A, Sikic BI, Shen X, Ramies DA, et al. Activity of cabozantinib (XL184) in advanced ovarian cancer patients (pts): results from a phase II randomized discontinuation trial (RDT). J Clin Oncol 29:15s, 2011 (suppl; abstr 5008).
48. Yasenchak C, Nackaerts K, Awada A, Gadgeel SM, Hellerstedt B, Perry MC, et al. Phase 2 results of XL184 in a cohort of patients (pts) with advanced non-small cell lung cancer (NSCLC). Eur J Cancer 2010;8:7. Abstract 397.
49. Van Cutsem E, Su WC, Davis J, Haas N, Samuel TA, Tsao CJ, et al. Phase 2 study of XL184 in a cohort of patients (pts) with hepatocellular carcinoma (HCC). Eur J Cancer 2010;8:7. Abstract 408.

Published OnlineFirst September 16, 2011; DOI: 10.1158/1535-7163.MCT-11-0264

AACR American Association for Cancer Research

Molecular Cancer Therapeutics

Cabozantinib (XL184), a Novel MET and VEGFR2 Inhibitor, Simultaneously Suppresses Metastasis, Angiogenesis, and Tumor Growth

F. Michael Yakes, Jason Chen, Jenny Tan, et al.

Mol Cancer Ther 2011;10:2298-2308. Published OnlineFirst September 16, 2011.